ELSEVIER

Journal of Chromatography A, 781 (1997) 251–261

JOURNAL OF CHROMATOGRAPHY A

Quaternary structural analysis of nucleoside diphosphate kinases using capillary electrophoresis

Yoo Jeong Heo[a], Sun Young Kim[a], Eunhee Kim[b], Kong-Joo Lee[a,*]

[a]*College of Pharmacy, Ewha Womans University, Seoul 120-750, South Korea*

[b]*Department of Genetic Engineering, Pai-Chai University, Taejon 302-735, South Korea*

Abstract

Capillary electrophoresis was used to monitor the quaternary structure and structural changes by denaturants of nucleoside diphosphate kinase (NDP kinase). NDP kinase from human erythrocyte consists of two kinds of polypeptide chains: A (Nm23-H1) and B (Nm23-H2), which are the products of nm23-H1 and -H2 genes, respectively. Structural characteristics of native NDP kinase, recombinant Nm23-H1 and -H2 were examined using capillary electrophoresis employing high pH running buffer in an uncoated fused-silica capillary as a separation column. The results were compared with those of the conventional sodium dodecyl sulfate and non-denaturing polyacrylamide gel electrophoresis. It shows that capillary electrophoresis is a possible tool to investigate protein structure, including the quaternary structure. This protocol was applied to the investigation of the denaturation process of each enzyme by denaturants (6 *M* urea or heating to 70°C) and to the monitoring of the interaction between denatured Nm23-H1 and -H2. The structural information of NDP kinase obtained by analysis using capillary electrophoresis is valuable for understanding its suggested biological function as a tumor metastasis suppressor and c-*myc* transcription factor, etc. © 1997 Elsevier Science B.V.

Keywords: Proteins; Enzymes; Nucleoside diphosphate kinases

1. Introduction

Capillary electrophoresis (CE) is an attractive analytical technique applicable to the structural studies of proteins instead of more laborious biochemical methods. The adsorption of multicharged proteins on the negatively charged surface of a fused-silica capillary column became a serious problem in the CE separation of proteins. Several strategies were developed to overcome the problems: (a) removing the negative charges of the capillary surface by using a lower pH running buffer than the pK_a of silanol (pH 2.5) [1], (b) using a higher pH than the isoelectric point (pI) of most proteins (>9.0) where the proteins would be negatively charged [2,3], (c) coating the inner surface of the capillary with a hydrophilic polymer [4]. These advances make it possible to analyze the small alterations of proteins with CE: the separation of metallothionein isoforms [5], and apo and holo proteins of ferritin [6], and serine hydroxymethyltransferase [7]. Monitoring the process of protein folding/unfolding as a function of the amount of denaturant provides information about the conformational stability of the molecules. The folding/unfolding transition and the possible unfolding intermediates, which cannot be seen in conventional urea gradient gel electrophoresis in urea because of the fast process, could be detected using CE: unfolding of human serum transferrin in urea [8] and thermally induced unfolding of lysozyme [9]. Recently, quantitative analysis of conformational

*Corresponding author.

0021-9673/97/$17.00
PII S0021-9673(97)00500-1

equilibrium in protein folding using CE has been reviewed by Hisler and Freire [10]. This review described theoretical approaches to the physical factors affecting the mobility of proteins, effects of the folding/unfolding isomerization process on the shape of the electrophoretic profile, and methodologies for determining the thermodynamic and kinetic parameters in each system. In this study, CE was used for examining the process of thermal- or urea-induced protein folding/unfolding of nucleoside diphosphate (NDP) kinases (Nm23s) having quaternary structure. The relationship between the structural change and enzymatic function was investigated.

NDP kinase catalyzes the transfer of the terminal phosphate group of the nucleoside triphosphate to the corresponding diphosphate ($N_1TP+N_2DP \rightarrow N_1DP+N_2TP$). The primary role of NDP kinase in the cell was considered as the maintenance of a pool of nucleoside triphosphates required for the biosynthesis. NDP kinases are highly conserved set of sequences throughout evolution from bacteria to humans. All of the sequences can be optimally aligned, with no insertion longer than one residue. Recently the interest in NDP kinases increased due to their identification as the products of nm23, a putative metastasis suppressor gene [11–13]. Two human NDP kinases have been identified as NDP kinase A (Nm23-H1) [14] and NDP kinase B (Nm23-H2) [15]. Nm23-H1 acts as a suppressor of metastasis for some tumor types [16]. Nm23-H2 was shown to be identical to PuF, a protein that binds to a nuclease-sensitive element in the promoter of c-*myc* oncogene, and activates transcription of the c-*myc* oncogene in vitro [17]. It turns out that NDP kinase activity is not required for its DNA binding [18]. Contradictory results on the function of the nm23 gene product have been presented. Reduced expression of Nm23 correlates with high metastatic potential in breast cancer [19], hepatocellular carcinoma [20], malignant melanoma [21] and gastric carcinoma [22]. On the other hand, high Nm23 expression has been reported to be associated with carcinogenesis or progression in colon carcinoma [23], neuroblastoma [24] and ovarian carcinoma [25]. The X-ray crystallographic structures of the NDP kinase from *Myxococcus xanthus* [26], *Dictyostelium discoideum* [27] and *Drosophila melanogaster* [28] have been reported. Although the overall topology of these structures is essentially identical, there are remarkable differences in the quaternary structure. Structural and solution studies of NDP kinases indicate that these enzymes are from either tetramers, as in NDP kinases from *M. xanthus*, yeast and rat, or hexamers, as in NDP kinase from *D. discoideum*, *Drosophila melanogaster* [29] and humans [30]. Nm23-H1 and Nm23-H2 are closely related in sequence (88% identical). Of the 18 residues that differ in the two sequences, seven involve replacements that result in an increase of net positive charge of Nm23-H2 relative to Nm23-H1. The calculated p*I* values of Nm23-H1 and Nm23-H2 are 6.13 and 8.64, respectively.

In this study, NDP kinase from human erythrocytes, recombinant Nm23-H1 and Nm23-H2 were purified and the native structure of each protein was characterized with CE. The results were compared with those of conventional sodium dodecyl sulfate (SDS) and non-denaturing polyacrylamide gel electrophoresis (PAGE). Changes of quaternary structure of Nm23 by heat or urea and the interaction of Nm23-H1 and Nm23-H2 were monitored with CE.

2. Experimental

2.1. Materials

Chemicals including urea, polyacrylamide, *N,N,N′,N′*-tetramethylethylenediamine (TEMED), ammonium persulfate, Trizma base (Tris), 4-(2-hydroxyethyl)-1-piperazineethanesulfonic acid (Hepes), ATP, UDP, $MgCl_2$, SDS, glycerol and β-mercaptoethanol (β-ME) were purchased from Sigma (St. Louis, MO, USA) and sodium borate from Kanto Chemicals (Tokyo, Japan). Radioisotope [γ-^{32}P]ATP was obtained from Amersham (Buckinghamshire, UK). The PEI cellulose TLC plate was from Alltech (Deerfield, IL, USA), and the ultrafiltration filter molecular mass cutoff 5000 from Millipore (Bedford, MA, USA).

2.2. Capillary electrophoresis procedure

For the protein analysis, the untreated fused-silica capillary (Polymicro Technologies, Phoenix, AZ, USA), 40 cm long (31.5 cm to detector)×50 μm I.D.

was used as a separation column. The apparatus used for these studies was an automated $HP^{3D}CE$ system (Hewlett-Packard, Palo Alto, CA, USA) with $HP^{3D}CE$ Chemstation for control and data acquisition. $HP^{3D}CE$ is equipped with a photodiode array UV detector, an automatic pressure or electrokinetic sample injector, an autosampler, a Peltier temperature controller, and a 30 kV high-voltage power supply. Prior to each run the capillary was rinsed with 0.1 *M* sodium hydroxide solution, distilled water and running buffer. The capillary was filled with high-pH running buffer, usually 20 m*M* sodium borate buffer, pH 9.64, as described previously [2]. The samples were introduced by hydrodynamic injection (4×10^3 Pa for 10 s) and run by applying a voltage of 20 kV at 25°C.

2.3. SDS and non-denaturing polyacrylamide gel electrophoresis

The protein patterns of NDP kinases were analyzed using SDS-PAGE under reducing conditions. The proteins were separated on a 10% polyacrylamide slab gel by the Laemmli procedure [31]. The gels were stained with Coomassie Brilliant blue. For the separation of native protein without denaturation, non-denaturing gel matrix was prepared, containing 36 m*M* Tris base, 36 m*M* boric acid, 0.8 m*M* EDTA (pH 8.3), 2.5% glycerol, 5% acrylamide with ammonium peroxide and TEMED. Protein samples (0.5 μg) were autophosphorylated with 0.5 μCi [γ-^{32}P]ATP in 10 ml reaction buffer (20 m*M* Hepes (pH 7.9), 5 m*M* $MgCl_2$, 0.1 m*M* EDTA, 1 m*M* dithiothreitol (DTT), 100 m*M* KCl, 3% glycerol) at 37°C for 20 min. Phosphorylated protein was separated at 100 V for 1 h on a 5% horizontal non-denaturing polyacrylamide gel. The protein bands were detected with autoradiography after drying.

2.4. NDP kinase assay

Enzyme activity was measured using a modified method as described previously [23,24]. Enzyme reaction was started by adding urea- or heat-treated sample in reaction buffer (10 μl) containing 20 m*M* Hepes (pH 7.4), 1 m*M* each ATP and UDP as substrate, 0.5 μCi [γ-^{32}P]ATP and 2 m*M* $MgCl_2$, incubated at 30°C for 10 min and stopped by adding gel sample buffer containing 125 m*M* Tris base, 2.3% SDS, 10% glycerol and 5% β-ME. Aliquots were loaded onto PEI cellulose TLC plates and developed in a solution of 0.75 *M* KH_2PO_4 (pH 3.4). The plate was dried and autoradiograhy carried out, or the spots on the plate were quantitated using a Packard instant imager (Meriden, CT, USA).

2.5. Sample preparations

NDP kinase was purified as a native form from human erythrocytes using affinity chromatography as described by Kim et al. [32]. Recombinant proteins of NDP kinase A (Nm23-H1) and NDP kinase B (Nm23-H2) were obtained in the same way as described above from *E. coli* strain BL21 (transformed with pET3C expression plasmids containing nm23-H1 or nm23-H2 which were gifts from Dr. P.S. Steeg) after induction of Nm23-H1 and -H2 as described previously [33]. Purified proteins were desalted using Sephadex G-25 column chromatography. Denatured proteins for CE were obtained by heating the enzymes at various temperature for 10 min or by incubating the proteins with 6 *M* urea for 10 min at 37°C and removing the excess urea with ultrafiltration (M_r cutoff <5000). Renaturation of proteins was monitored with CE by reincubation of the samples at room temperature for a longer time.

3. Results and discussion

Structural characteristics of hexameric NDP kinase isoforms in native and in denatured condition were investigated using CE. The progress of the interaction between two isoforms under thermally denatured conditions could be monitored using CE; this is difficult to detect by other analytical methods.

3.1. Structural characterizations of native NDP kinase from human erythrocyte, recombinant Nm23-H1 and -H2 using CE and conventional PAGE

NDP kinase from human erythrocytes, consisting of two kinds of polypeptide chain A and B, recombinant Nm23-H1 (NDP kinase A) and Nm23-H2 (NDP

kinase B), were purified as described in Section 2, and separated on SDS-PAGE under reducing conditions according to the molecular mass of each subunit (see Fig. 1A). The monomer size of each protein was found to be M_r 17×10^3 and 19×10^3. The separation of each protein was performed using CE in an uncoated fused-silica capillary using high-pH running buffer (20 m*M* sodium borate buffer, pH 9.6) as described previously [2]. Capillary electropherograms of NDP kinase from human erythrocytes, Nm23-H1 and -H2 are presented in Fig. 1B. The separation order of these isoforms reflects the difference between net surface charge densities. The results agreed well with the calculated isoelectric point (p*I*) values of Nm23-H1 (p*I*=6.13) (Fig. 1B-a) and -H2 (p*I*=8.64) (Fig. 1B-b); the more basic protein, Nm23-H2, migrated faster towards the cathode. Each recombinant Nm23-H1 and -H2 has a homogeneous population presumed to be A_6 or B_6, as described previously [30]. When the same amounts of recombinant Nm23-H1 and -H2 were mixed and incubated at 37°C, the CE pattern was same as the addition of either Nm23-H1 and -H2 (Fig. 1B-c). This means there was no interaction between two native recombinant proteins. The separation profile of native NDP kinase from human erythrocytes using CE is shown in Fig. 1B-d. Native NDP kinase, which has an identical SDS-PAGE pattern as the mixture of Nm23-H1 and -H2 gave five main peaks between Nm23-H1 and -H2 in the capillary electropherogram. This indicates that native NDP kinase has heterogeneous populations. The possible structure of native NDP kinase could be presumed from the migration order in CE; multimeric proteins composed of various combinations of NDP kinase A and B having different p*I* values (AB_5, A_2B_4, A_3B_3, A_4B_2 and A_5B). This is clear evidence to support the hypothesis that native human erythrocyte NDP kinase has a heterohexameric structure, which was suggested previously from the molecular weight obtained using gel filtration column chromatography [30]. The determination of isoform population was possible using CE; A_3B_3 was the main peak and A_6 or B_6 were not detectable under native conditions. The UV absorbance spectrum of each peak in CE was similar, regardless of the isoform combination (Fig. 1C). The isoform profile in CE was confirmed by comparison with that on non-denaturing PAGE based on the isoelectric points, as shown in Fig. 1D. Native human erythrocyte NDP kinase exhibited five bands which were consistent with the results obtained using CE, Nm23-H1 or -H2 generated single bands on non-denaturing PAGE according to the isoelectric points of proteins. Even though the separation pattern of recombinant Nm23-H1, -H2 and human erythrocyte NDP kinase in capillary electropherogram was completely different, the enzyme activity of each isoform was similar and the stability varied [34,35]. The observed results suggest that the maintenance of protein tertiary structure around active site of isoforms is necessary for the enzyme activity, and the difference in quaternary structure detected with CE may not be involved in enzyme activity but be in enzyme stability and other biological functions. This is an example showing that CE is a suitable analytical tool for the determination of the quaternary structure of proteins.

3.2. Monitoring the structural changes of proteins by urea and thermal denaturation

When Nm23-H1, -H2, the mixture of Nm23-H1 and -H2, and human erythrocyte NDP kinase were incubated with 6 *M* urea at 37°C for 10 min and excess urea was removed by ultrafiltration, the denatured proteins were eluted between Nm23-H1 and -H2 in the capillary electropherogram (Fig. 2A). The Nm23-H2 peak disappeared in the presence of 6 *M* urea, which might be caused by protein aggregation or adsorption onto the capillary wall (Fig. 2A-c). An interaction between urea-denatured Nm23-H1 and -H2 (1:1) can be observed in Fig. 2A-d, even though the association of Nm23-H1 and -H2 under native conditions was negligible. The products obtained from this association were not well resolved and had similar capillary electropherograms as that of denatured NDP kinase, as shown in Fig. 2A-d. This shows that the interaction between Nm23-H1 and -H2 and quaternary structural changes occur only under unfolding conditions after denaturation. The quaternary structural changes can be easily detected by analysis using CE. This interaction between Nm23-H1 and -H2 might be random association, but the exact conformation could not be explained with CE data. However, it is possible to suggest that serious conformational changes with

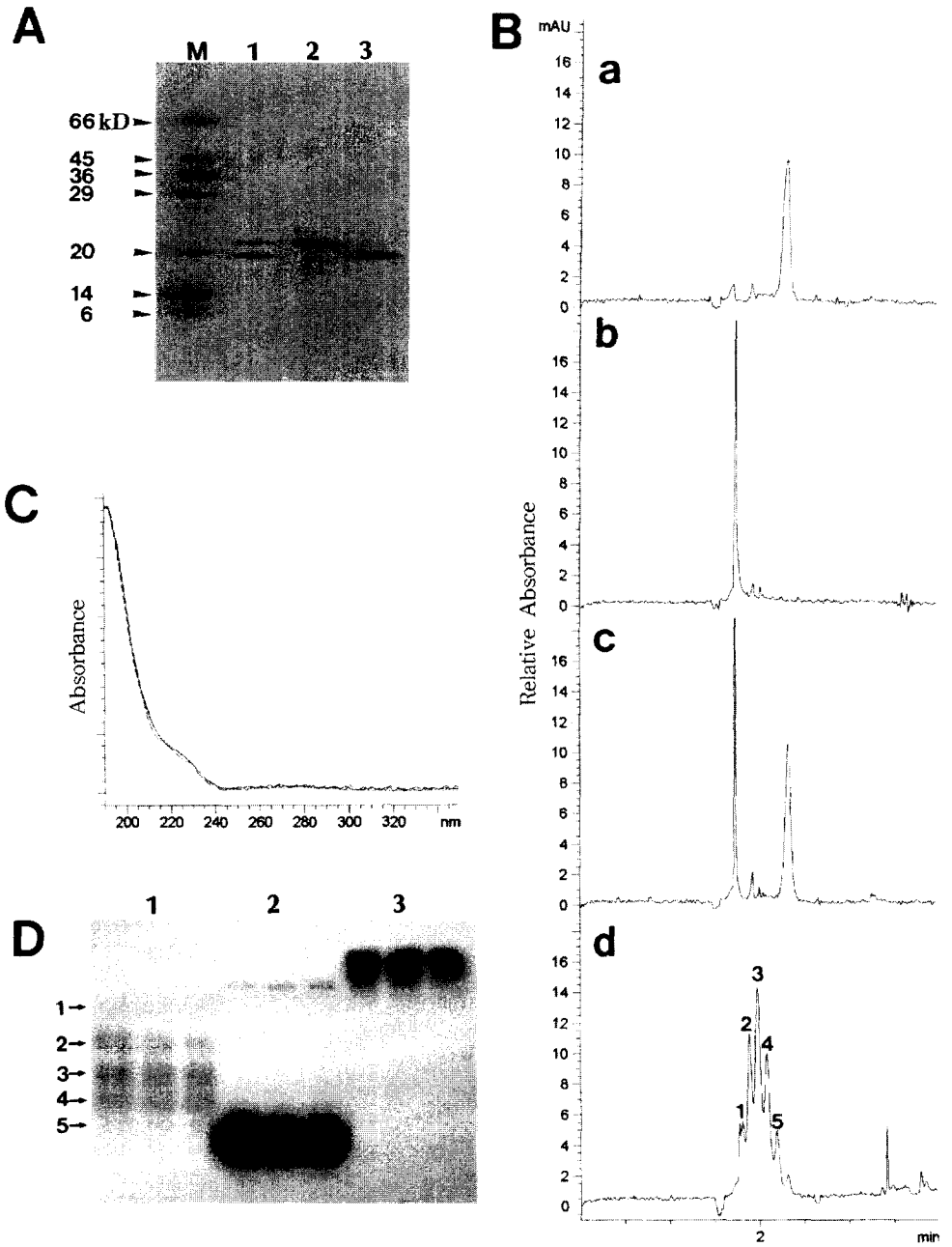

Fig. 1. (A) Separation of purified NDP kinase from human erythrocyte (lane 1), recombinant Nm23-H1 (lane 2) and Nm23-H2 (lane 3) on 13% SDS-PAGE under reducing conditions based on molecular mass kD, kilodalton. (B) Separation of purified recombinant Nm23-H1 (a), Nm23-H2 (b), mixture of recombinant Nm23-H1 and -H2 (c) and NDP kinase from human erythrocyte (d) with capillary electrophoresis in a 40-cm (31.6 cm to UV detector)×50 μm I.D. bared fused-silica column. CE conditions were the following: running buffer, 20 m*M* sodium borate buffer (pH 9.6); applied voltage, 20 kV; temperature, 25°C; injection, by pressure at 4×10^3 Pa for 10 s; detection wavelength, 200 nm. (C) UV absorbance spectrum of each peak in the capillary electropherogram in (B) monitored by diode array detection. (D) Autoradiogram of autophosphorylated native NDP kinase with [γ-^{32}P]ATP (lane 1), recombinant Nm23-H1 (land 2) and -H2 (land 3) separated on 5% non-denaturing PAGE.

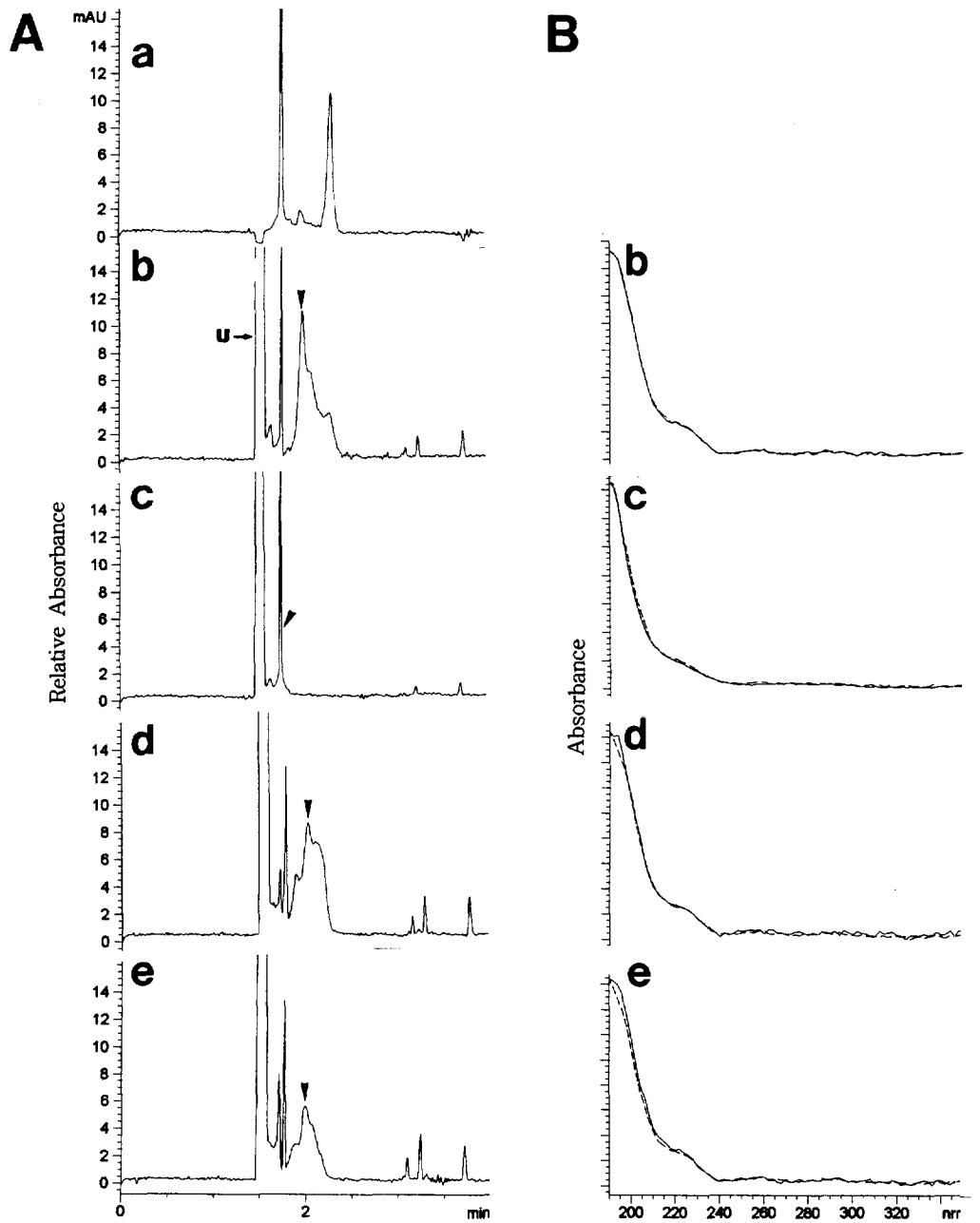

Fig. 2. (A) Capillary electropherograms of proteins after incubating with 6 *M* urea at 37°C or 10 min. CE conditions as in Fig. 1B. (a) Control mixture of recombinant Nm23-H1 and -H2, (b–e) urea denatured proteins: (b) Nm23-H1, (c) Nm23-H2, (d) mixture of Nm23-H1 and -H2, and (e) NDP kinase from human erythrocyte. (B) Comparison of UV absorbance spectrum between native (——) and urea-denatured (– – –) protein peaks at indicated arrow heads. U indicates the urea peak.

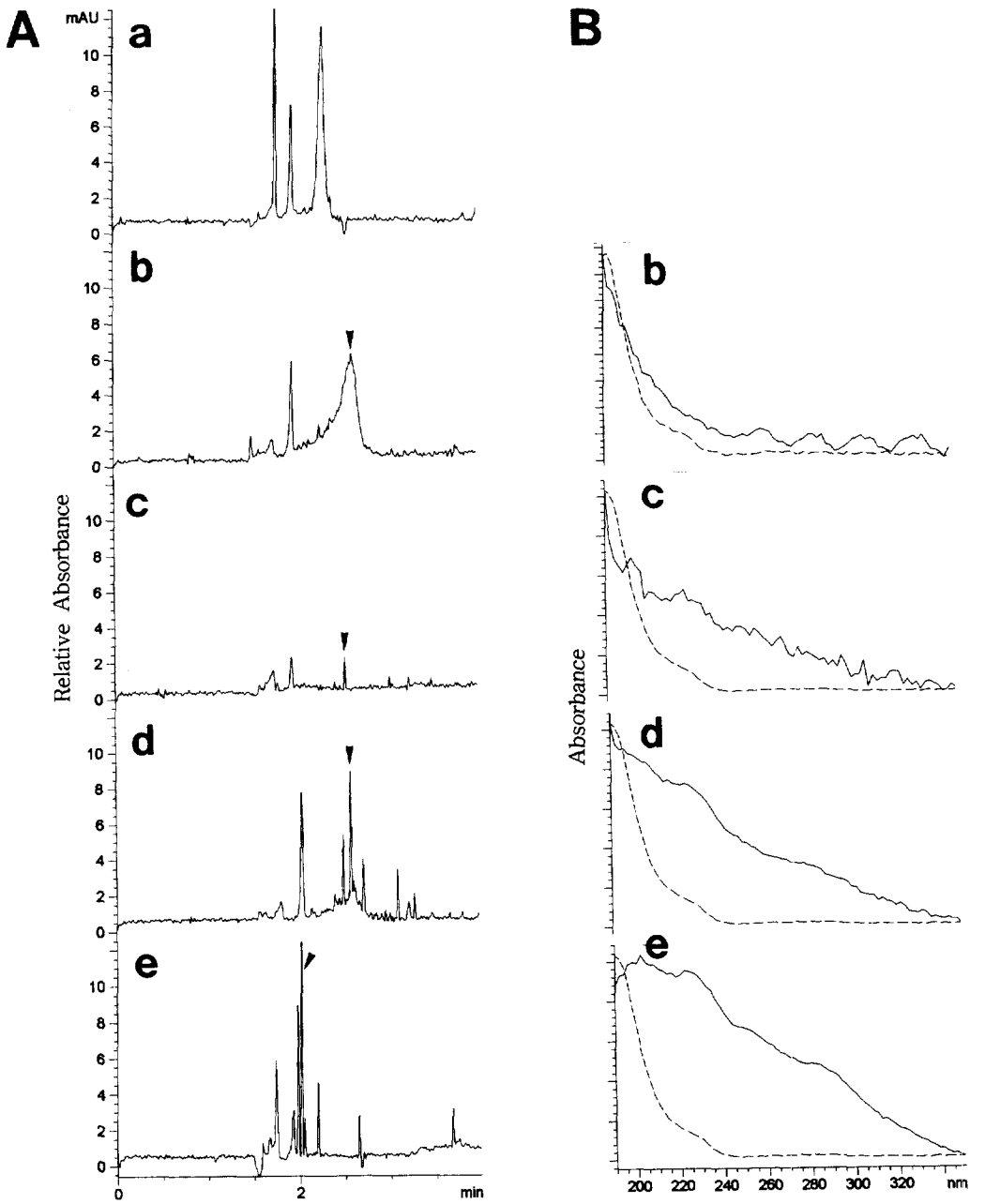

Fig. 3. (A) Capillary electropherograms of thermally denatured proteins at 70°C for 10 min. CE conditions were the same as in Fig. 1B. (a) Control mixture of recombinant Nm23-H1 and -H2 at 37 or 50°C. (b–e) Thermally denatured form at 70°C: (b) Nm23-H1, (c) Nm23-H2, (d) mixture of Nm23-H1 and H2, and (e) NDP kinase from human erythrocytes. (B) Comparison of UV absorbance spectrum between native (– – –) and thermally denatured (——) protein peaks at indicated arrows.

urea denaturation did not occur from the observation of no dramatic changes in UV absorbance spectra by urea-denatured proteins (see Fig. 2B). To examine the relationship between structural changes and the protein function, the enzyme activities in urea-treated samples were measured. Over 50% of enzyme activity was retained (data not shown). This indicates that conformational changes of urea-treated proteins, which do not show dramatic mobility changes in CE, were not enough for serious damage to active sites of the enzyme.

The thermal denaturation patterns of Nm23-H1, -H2, the mixture of Nm23-H1 and -H2, and NDP kinase were examined using CE (Fig. 3). Each enzyme was incubated at 37–70°C for 10 min and reincubated at room temperature for various times. Denaturation was not detected in CE at 50°C, so incubation at 70°C was adopted for thermal denaturation. The mobilities of thermally denatured samples (Fig. 3A-b–d) were less than those of native samples. In the case of NDP kinase from human erythocytes (Fig. 3A-e), the mobility was not changed, even though the resolved peak profile was completely different. The peak of denatured Nm23-H1 was broadened, as shown Fig. 3A-b, and sharp peaks were obtained in Nm23-H2, the mixture of Nm23-H1 and -H2, and native NDP kinase (Fig. 3A-c–e). The elution profile changes in Nm23-H1 or -H2 could not be detected depending on the reincubation time (Fig. 3A-b,c), and those in the mixture of Nm23-H1 and -H2 or human erythrocyte NDP kinase were varied during reincubation time (Fig. 3A-d,e). This indicates that the interactions between thermally denatured Nm23-H1 and -H2 were slow enough to detect using CE, and several intermediate conformations gained by the interaction were well resolved in the capillary electropherogram. UV absorbance spectra of thermally denatured enzymes were dramatically changed and the spectra obtained from various peaks were similar to each other (Fig. 3B). The remained enzyme activity of each sample after thermal denaturation are presented in Table 1. Human erythrocyte NDP kinase activity was most easily lost (by 30%), in the case of Nm23-H2, about 70% of enzyme activity remained, even though the peaks became smaller in the capillary electropherogram (Fig. 3A-c).

The electrophoretic mobility is expected to be different for the various structural states due to the changes in the valence, size, shape, and degree of hydration associated with each state. The results indicate that proteins denatured using different denaturants have different electrophoretic mobilities, even if the precise origin of these differences cannot be evaluated. A decrease in mobility of the thermally denatured form may predominantly be due to the expansion of the molecule, which could induce the dramatic change in the UV absorbance spectrum (Fig. 3B). An increase in mobility of the urea-denatured form may due to the increase in valance. Monitoring the interaction of denatured Nm23-H1 and -H2 using CE could give useful information for understanding the relationship between structure and biological function.

3.3. Monitoring the progress of interaction between thermally denatured Nm23-H1 and -H2 at various stoichiometric ratios

To investigate the interaction between Nm23-H1 and -H2, samples containing various ratios of Nm23-H1 and -H2 were denatured at 70°C and reincubated at room temperature for various times. The elution profiles of interaction products in CE were entirely different depending on the ratio of Nm23-H1 and -H2, as shown in Fig. 4. When the ratio of Nm23-H1 to -H2 was 1:5, two main peaks were observed immediately after heating at 70°C (Fig. 4A-b), and

Table 1
Remaining enzyme activity after thermal denaturation at 70°C for 10 min

Protein	Enzyme activity (%)
Control native enzyme	100.0
NDP kinase after thermal denaturation	29.6
Recombinant Nm23-H1 after thermal denaturation	42.1
Recombinant Nm23-H2 after thermal denaturation	77.5

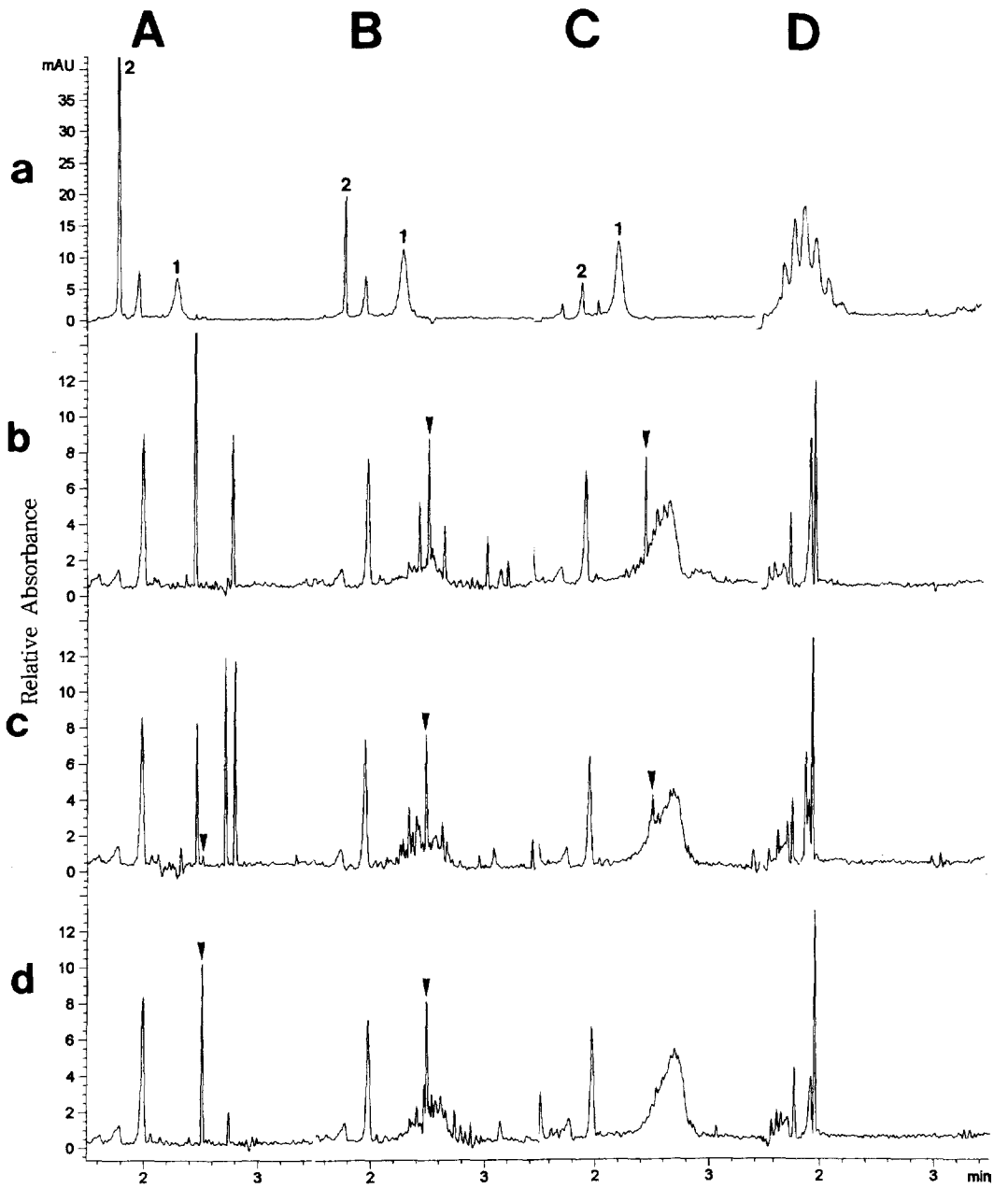

Fig. 4. Monitoring the interaction between thermally denatured Nm23-H1 and -H2 at various stoichiometries; (A) H1:H2, 1:5; (B) H1:H2, 1:1; (C) H1:H2, 5:1; and (D) human erythrocyte NDP kinase. Each sample was thermally denatured at 70°C for 10 min and reincubated at room temperature for various times: (a) control sample, (b) 0 min, (c) 54 min and (d) 108 min. CE conditions as in Fig. 1B.

intermediates appeared and disappeared during incubation at room temperature (Fig. 4A-b–d). After 2 h, one conformation was obtained on reaching the equilibrium state (Fig. 4A-d), which was similar to the peak obtained from Nm23-H2 itself. In Fig. 4B, fewer intermediate peaks appeared when mixing the

same amount of Nm23-H1 and -H2, and reached the equilibrium state quickly. With an excess amount of Nm23-H1 compared to -H2 (5:1), a sharp peak proposed to contain -H2 appeared immediately after heating, and diluted to the broad denatured Nm23-H1 peak during incubation.

The thermal denaturation of native protein composed of one kind of polypeptide occurred quickly, and no intermediate was observed, as shown in Fig. 3B-b,c, on the other hand, the association process of Nm23-H1 and -H2 was slow enough to detect using CE, and the shape of the electrophoretic profile was changed during incubation (Fig. 4-b,d). It is necessary to consider the factors affecting the shape of the electrophoretic profile. The decrease of electrophoretic mobility in the denatured form (Fig. 3) was mainly due to the changes of the mobilities and diffusion properties in the unfolded state. The shape of the electrophoretic profile after the association of Nm23-H1 and -H2 (Fig. 4) may be dependent on the kinetics of the isomerization process, as described previously [36]. The associated proteins can exist in a variety of different conformational states depending the molar ratio of Nm23-H1 and -H2 (Fig. 4b,c). The intermediate states which become only marginally populated have disappeared, and one conformation was obtained at the equilibrium state (Fig. 4d). Final conformations were identified as the denaturation states by examining the absorbance spectra, which were same as those in Fig. 3A-d (data not shown). The shape of the electrophoretic profile of intermediate or equilibrium state depended on the ratio of Nm23-H1 and -H2, as shown Fig. 4d.

4. Conclusions

This study demonstrates the utility of CE for monitoring the quaternary structure and structural changes by denaturants of NDP kinase. Structural characteristics of native NDP kinase consisting of two kinds of polypeptide chain A and B, recombinant Nm23-H1 and -H2, were examined using CE, by employing a high-pH running buffer in an uncoated fused-silica capillary as a separating column. The results were compared with those of conventional SDS and non-denaturing polyacrylamide gel electrophoresis. It shows that CE is a possible tool to investigate the protein structure, including the quaternary structure. This protocol was extended for examining the denaturation process of each enzyme by denaturants (6 *M* urea or 70°C heating) and for monitoring the interaction between denatured Nm23-H1 and -H2. The origin of this interaction could not be explained with the results obtained using CE, but monitoring the structural changes using CE can show the protein conformational states. The structural information about NDP kinase obtained using CE analysis could be valuable for understanding the suggested biological functions as a tumor metastasis suppressor and transcription factor, etc.

Acknowledgments

This research was supported by the grant from KOSEF (95-0403-25-02-2 and 951-0304-028-2) and MOE (No. 135). We thank Dr. P.S. Steeg at NCI for providing the expression plasmids pET3C-nm23-H1 and pET3C-nm23-H2.

References

[1] R.M. McCormick, Anal. Chem. 60 (1988) 2322–2328.
[2] K.-J. Lee, G.S. Heo, J. Chromatogr. 559 (1991) 317–324.
[3] J.W. Kim, J.H. Park, J.W. Park, H.J. Doh, G.S. Heo, K.-J. Lee, Clin. Chem. 39 (1993) 689–692.
[4] S. Hjerten, J. Chromatogr. 347 (1985) 191–198.
[5] J.H. Beattie, M.P. Richards, J. Chromatogr. A 700 (1995) 95–103.
[6] Z. Zhao, A. Malik, M.L. Lee, G.D. Watt, Anal. Biochem. 218 (1994) 47–54.
[7] M.A. Strege, D.F. Schmidt, A. Kreuzman, J. Dotzlaf, W.K. Yeh, R.E. Kaiser, A.L. Lagu, Anal. Biochem. 223 (1994) 198–204.
[8] V.J. Hisler, G.D. Worosila, E. Freire, Anal. Biochem. 208 (1993) 125–131.
[9] F. Kilar, S. Hjerten, J. Chromatogr. 638 (1993) 269–276.
[10] V.J. Hisler, E. Freire, Anal. Biochem. 224 (1995) 465–485.
[11] A. Leone, U. Flatow, C. Richter-King, M.A. Sandeen, I.M.K. Margulies, L.A. Liotta, P.S. Steeg, Cell 65 (1991) 26–34.
[12] P.S. Steeg, G. Bevilacqua, L. Kopper, J. Thorgeirsson, E. Talmadege, L. Liotta, M. Sobel, J. Natl. Cancer Inst. 80 (1988) 200–204.
[13] P.S. Steeg, F.M. Bevilacqua, R. Pozzatti, L.A. Liotta, M.E. Sobel, Cancer Res. 48 (1988) 6550–6554.

[14] A.M. Rosenfard, H.C. Krutzsch, A. Shearn, J.R. Biggs, E. Barker, I.M.K. Margulies, C.R. King, L.A. Liotta, P.S. Steeg, Nature 342 (1989) 177–180.
[15] J.A. Stahl, A. Leone, A.M. Rosengard, L. Porter, C.R. King, P.S. Steeg, Cancer Res. 51 (1991) 445–449.
[16] A. De La Rosa, R.L. Williams, P.S. Steeg, Bioessays 17 (1995) 53–62.
[17] E.H. Postel, S.J. Berberich, S.J. Flint, C.A. Ferrone, Science 261 (1993) 478–480.
[18] E.H. Postel, C.A. Derrone, J. Biol. Chem. 269 (1994) 8627–8630.
[19] R. Barns, S. Masood, E. Barker, A.M. Rosengard, D.L. Coggin, T. Crowell, C.R. King, K. Porter-Jordan, E. Wargotz, L.A. Liotta, P.S. Steeg, Cell 63 (1991) 933–940.
[20] T. Nakayama, A. Ohtsuru, K. Nakao, M. Shima, K. Nakata, K. Watanabe, K. Ishii, N. Kimura, S. Nagataki, J. Natl. Cancer Inst. 84 (1992) 1349–1354.
[21] V.A. Florenes, S. Aamdal, O. Myklebost, G.M. Maelandsmo, O.S. Bruland, O. Fodstad, Cancer Res. 52 (1992) 6088–6091.
[22] H. Nakayama, W. Yasui, H. Yokozaki, E. Tahara, Cancer Res. 84 (1993) 184–190.
[23] M. Haut, P.S. Steeg, J.K.V. Willson, S.D. Markowitz, J. Natl. Cancer Inst. 83 (1991) 712–716.
[24] N. Hailat, D.R. Keim, R.F. Mehem, X.X. Zhu, C. Eckerskorn, G.M. Brodeur, C.P. Reynolds, R.C. Seeger, F. Lottspeich, J.R. Strahler, S.M. Hanash, J. Clin. Invest. 88 (1991) 341–345.
[25] M. Mandai, I. Konishi, M. Koshiyama, T. Mori, S. Arao, H. Tahiro, H. Okamura, H. Nomura, M. Fukumoto, Cancer Res. 54 (1994) 1825–1830.
[26] R.L. Williams, D.A. Oren, J. Munoz-Dorado, S. Inouye, M. Inouye, E. Arnold, J. Mol. Biol. 234 (1993) 1230–1247.
[27] S. Morera, G. LeBras, I. Lascu, M.L. Lacombe, M. Veron, J. Janin, J. Mol. Biol. 243 (1994) 873–890.
[28] M. Chiadmi, S. Morera, I. Lascu, C. Dumas, D. Le Bras, M. Veron, J. Janin, Structure 15 (1993) 283–293.
[29] P.A. Webb, O. Perisic, C.E. Mencola, J.M. Backer, R.L. Williams, J. Mol. Biol. 251 (1995) 574–587.
[30] A.-M. Gilles, E. Presecan, A. Vonica, I. Lascu, J. Biol. Chem. 266 (1991) 8784–8789.
[31] U.K. Laemmli, Nature (London) 227 (1979) 680–685.
[32] S.Y. Kim, J.A. Chung, H.J. Doh, E. Kim, K.-J. Lee, Mol. Cell., in press.
[33] N.J. MacDonald, A. De La Rosa, M.A. Benedict, J.M.P. Freije, J. Krutsch, P.S. Steeg, J. Biol. Chem. 268 (1993) 25780–25789.
[34] J. Munoz-Dorado, N. Almaula, S. Inouye, M. Inouye, J. Bacteriol. 175 (1993) 1176–1181.
[35] S.Y. Kim, E. Kim, K.-J. Lee, in preparation.
[36] J.R. Cann, J.G. Kirkwood, R.A. Brown, Arch. Biochem. Biophys. 72 (1957) 37–41.